LEMIEUX, R. U. & CHU, P. (1958). *Abstr. Am. Chem. Soc. Meet.* **133**, 31N.
LEMIEUX, R. U., KOTO, S. & VORSIN, D. (1979). *Anomeric Effect. Origin and Consequences*, ACS Symposium Series 87, edited by W. A. SZARAK & D. HORTON. Washington, DC: American Chemical Society.
LEMIEUX, R. U. & PAVIA, A. A. (1969). *Can. J. Chem.* **47**, 4441–4446.
LESYNG, B., JEFFREY, G. A. & MALUSZYNSKA, H. (1988). *Acta Cryst.* B**44**, 193–198.
LIS, T. (1983). *Carbohydr. Res.* **122**, 23–29.
LLEWELLYN, F. J., COX, E. G. & GOODWIN, T. H. (1937). *J. Chem. Soc.* pp. 883–894.
LONGCHAMBON, F., GILLIER-PANDRAUD, R., WEIST, R., REES, B., MITSCHLER, A., FELD, R., LEHMAN, M. S. & BECKER, P. (1985). *Acta Cryst.* B**41**, 47–56.
NOLLER, C. R. & ROCKWELL, W. C. (1938). *J. Am. Chem. Soc.* **60**, 2076–2077.
PANAGIOTOPOULOS, N., JEFFREY, G. A., LAPLACA, S. & HAMILTON, W. C. (1974). *Acta Cryst.* B**30**, 1421–1430.
PARK, Y. J., JEFFREY, G. A. & HAMILTON, W. C. (1971). *Acta Cryst.* B**27**, 2393–2401.
PEREZ, S., PIERRE, ST. & MARCHESSAULT, R. (1978). *Can. J. Chem.* **56**, 2866–2871.
PFEFFER, P. E. (1984). *J. Carbohydr. Chem.* **3**, 613–639.
PICHON-PESME, V. & HANSEN, N. K. (1989). *J. Mol. Struct. (Theochem.)*, **183**, 151–160.
PIGMAN, W. (1957). Editor. *The Carbohydrates: Chemistry, Biochemistry and Physiology*. New York: Academic Press.
PIGMAN, W. & HORTON, D. (1970). Editors. *The Carbohydrates: Chemistry and Biochemistry*. New York: Academic Press.
PIMENTEL, G. C. & MCCLELLAND, A. L. (1960). *The Hydrogen Bond*. San Francisco: W. H. Freeman.
Rodd's Chemistry of Carbon Compounds (1967). 2nd ed., edited by S. COFFEY. Supplement FG (1983), edited by M. F. ANSELL. Amsterdam: Elsevier.
RUBLE, J. & JEFFREY, G. A. (1974). *Carbohydr. Res.* **38**, 61–69.
SAENGER, W. (1979). *Nature (London)*, **279**, 343–344.
SAENGER, W. (1982). *Nature (London)*, **296**, 581–583.
SAENGER, W. (1984). *Inclusion Compounds*, edited by J. L. ATWOOD, J. E. D. DAVIES & D. D. MACNICOL, pp. 231–259. New York: Academic Press.
SASTRY, D. L., TAKEGOSHI, K. & MCDOWELL, C. A. (1987). *Carbohydr. Res.* **165**, 161–171.
SAVAGE, H. & FINNEY, J. (1986). *Nature (London)*, **322**, 717–720.
SENMA, M., TAIRA, Z., OSAKI, K. & TAGA, T. (1973). *J. Chem. Soc. Chem. Commun.* p. 880.
STODDARD, J. F. (1971). *Stereochemistry of Carbohydrates*. New York: Wiley.
SUNDARALINGAM, M. (1969). *Biopolymers*, **7**, 821–830.
TVAROSKA, I. & PEREZ, S. (1986). *Carbohydr. Res.* **149**, 389–410.
WOLFE, S. (1972). *Acc. Chem. Res.* **5**, 102–111.
WOOD, R. A., JEFFREY, G. A., PFEFFER, P. E. & HICKS, K. B. (1983). *J. Am. Chem. Soc.* **105**, 2128–2133.

Acta Cryst. (1990). B**46**, 103–111

Electron Microscopy Study of the Structure of Metastable Oxides Formed in the Initial Stage of Copper Oxidation. V. $Cu_4O_{0.75}$*

BY R. GUAN

Laboratory of Atomic Imaging of Solids, Institute of Metal Research, Academia Sinica, 110015 *Shenyang, People's Republic of China*

H. HASHIMOTO

Faculty of Engineering, Okayama University of Science, Okayama 700, *Japan*

AND K. H. KUO

Beijing Laboratory of Electron Microscopy, Academia Sinica, PO Box 2724, *Beijing, People's Republic of China*

(*Received* 22 *June* 1988; *accepted* 18 *September* 1989)

Abstract

Besides Cu_4O, Cu_4O-S_1 and Cu_4O-S_2 reported previously, three allotropes of a new metastable oxide of copper, α-$Cu_4O_{0.75}$, β-$Cu_4O_{0.75}$ and γ-$Cu_4O_{0.75}$, have been observed by high-resolution electron microscopy in an early stage of the oxidation of copper. The atomic positions of Cu and O have been determined by comparing the observed structure images with simulated ones calculated using the theories of electron diffraction and image formation. These new suboxides have oxygen-deficient Cu_4O structures and the O atoms occupy not only the central positions in the tetrahedra consisting of four Cu atoms, but also the central positions in the octahedra consisting of six Cu atoms. The differences between α-, β- and γ-$Cu_4O_{0.75}$ are due to the distribution of O atoms.

* Project partly supported by the National Natural Science Foundation of the People's Republic of China, under grant 888600.

0108-7681/90/020103-09$03.00

1. Introduction

A series of metastable suboxides with the chemical compositions Cu_4O (Guan, Hashimoto & Yoshida, 1984), Cu_4O-S_1, Cu_4O-S_2 (Guan, Hashimoto, Kuo & Yoshida, 1987), Cu_8O (Guan, Hashimoto & Kuo, 1984) and $Cu_{64}O$ (Guan, Hashimoto & Kuo, 1985), formed in the initial stage of the oxidation of copper, have been observed using a high-resolution electron microscope (HREM). The oxygen content of the Cu_4O-S_1 and Cu_4O-S_2 superstructures is the same as that in Cu_4O, but the positions of the O atoms are different (Guan, Hashimoto, Kuo & Yoshida, 1987). In Cu_4O, the O atoms are all situated in the center of tetrahedra consisting of four Cu atoms, whereas the Cu_4O-S_1 and Cu_4O-S_2 structures consist of three unit cells of Cu, each of which has O atoms partly situated in tetrahedra and partly situated in octahedra of Cu atoms.

Structure determinations of Cu_4O, Cu_4O-S_1, Cu_4O-S_2, Cu_8O and $Cu_{64}O$ have been carried out by studying electron diffraction patterns and electron microscope observations of the structure images projected parallel to the *a*, *b* and *c* axes, and comparing

Fig. 1. Thin copper-oxide films formed on a copper substrate.

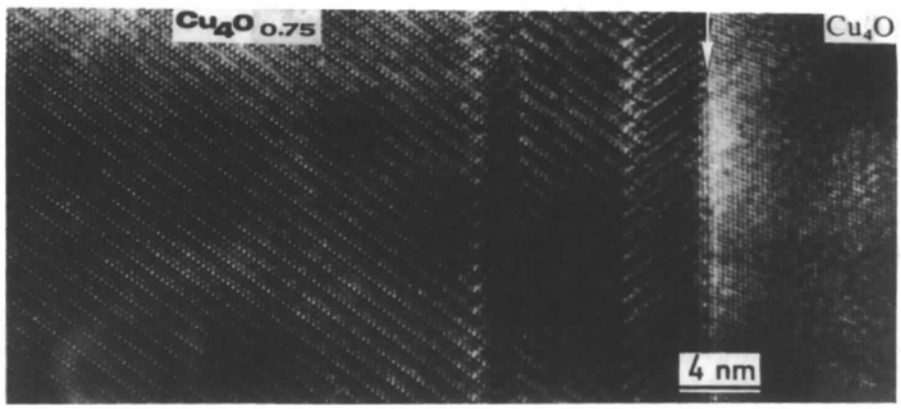

Fig. 2. Image of Cu_4O_x with twin structure adjacent to Cu_4O. The arrow shows the boundary between Cu_4O and Cu_4O_x.

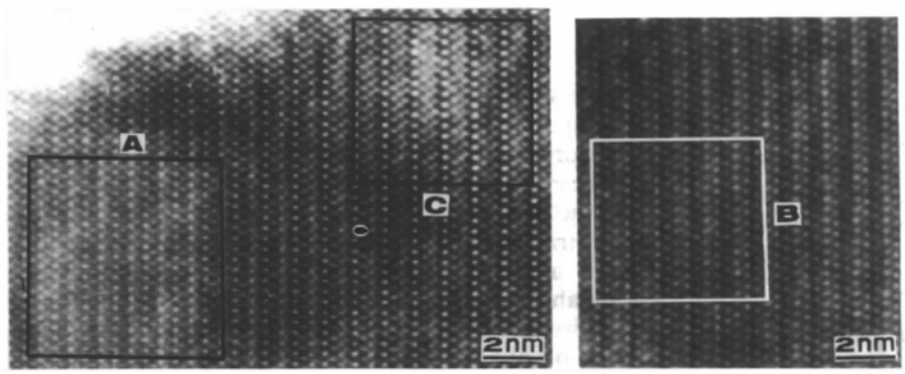

Fig. 3. HREM image showing Cu_4O with different contrast: regions *A*, *B* and *C*.

these observations with the diffraction intensity distribution and image contrast calculated by electron diffraction and image-formation theories.

The present paper reports three further structures of the Cu_4O family, α-$Cu_4O_{0.75}$, β-$Cu_4O_{0.75}$ and γ-$Cu_4O_{0.75}$. These oxides were formed in different small regions of about 6 to 15 nm thickness in a Cu_4O thin film of 300 nm^2 area. Since the areas of the specimen regions are very small and it is rather difficult to take structure images of each area in more than two directions, the positions of the atoms have been proposed from investigations of the contrast of the images projected onto the *ab* plane and from the possible O-atom positions along the *c* axis.

2. Experimental

A rolled copper plate of 60–70 μm thickness was electropolished by the open-window method into a thin film with a thickness of about 20 nm, suitable for observation by high-resolution electron microscopy. The thin film was then oxidized at 770–820 K in a vacuum of 2–2·4 Pa for about 2 min. The oxides of different structure were produced in parts of the film with different thickness even when the oxidation conditions were the same for all areas of the specimen. The electron diffraction patterns and the HREM images at an atomic level were recorded using a JEM-100CX electron microscope.

3. Results

Fig. 1 shows a low-magnification electron microscope image of copper oxide films grown on a Cu crystal. The dark region in the lower part of this figure is the Cu film and the thin region at the top is the formed copper oxides, shown by electron diffraction to be Cu_4O. The HREM images of these oxide films show various contrasts in the different regions, some of which have been analyzed previously to be Cu_4O, Cu_4O-S_1 and Cu_4O-S_2 (Guan, Hashimoto & Yoshida, 1984; Guan, Hashimoto, Kuo & Yoshida, 1987). However, these films, which were prepared under the same conditions, contained regions whose structure had not been analyzed. The unknown structure was tentatively denoted Cu_4O_x.

Crystals with the Cu_4O_x structure are often formed in a region adjacent to the Cu_4O crystal region, sometimes with twin structure as shown in Fig. 2. To the right of the twin boundary, indicated by an arrow, a uniform Cu_4O structure of [001] orientation is seen while to the left of the boundary the Cu_4O_x structure is seen.

Fig. 3 shows large-magnification HREM images of Cu_4O_x. The images were taken from the left side of Fig. 2, but far away from the twin boundary. One of the selected-area electron diffraction patterns from an area shown in Fig. 3 is shown in Fig. 4. Even though the positions of the selected areas were changed, the corresponding diffraction patterns did not show a noticeable change which seems to be due to the large aperture size of area selection. However, the images shown in regions *A*, *B* and *C* of Fig. 3 show different contrast. Since these areas were oxidized under the same conditions, they can be expected to have a chemical composition similar to Cu_4O. Thus the composition was tentatively assumed to be Cu_4O_x, where x is an unknown value close to 1.

Fig. 5 schematically shows a comparison of the electron diffraction patterns of Cu_4O_x, Cu_4O and Cu. The dots in the figure represent the diffraction spots from Cu_4O_x, the small circles represent the spots from Cu_4O in the [001] orientation and the large circles represent the spots from Cu in the [011] orientation. It can be seen from Fig. 5 that all of the diffraction spots of Cu_4O are superposed with those of Cu_4O_x, but Cu_4O_x has two times more spots in the [010] Cu_4O direction than Cu_4O has, whereas in the [100] Cu_4O direction both structures have the same number of spots. These facts clearly suggest that the basic period of the Cu_4O_x structure is twice as large as that of Cu_4O in the [010] Cu_4O direction but the same in the [100] Cu_4O direction. As was reported previously (Guan, Hashimoto & Yoshida, 1984), the [001] orientation of Cu_4O corresponds to the [01$\bar{1}$] orientation of Cu, thus the diffraction spots of Cu(200) and (111) should be superposed with (200) and (120) diffraction spots of Cu_4O if the distortion in the crystal lattice caused by the inclusion of the interstitial O atoms in the copper lattice is negligibly small.

In the images labelled *A*, *B* and *C* in Fig. 3, the contrast of the white dots changes in an abrupt and

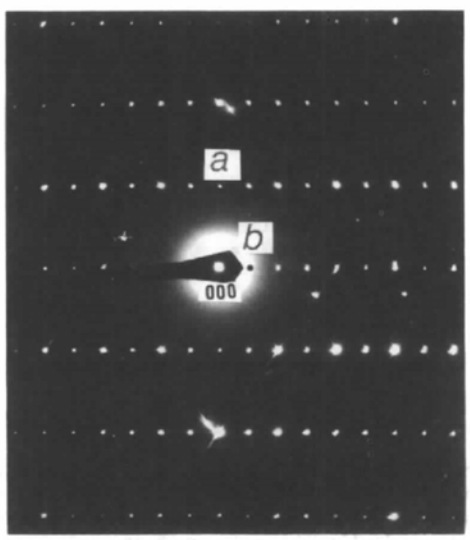

Fig. 4. Electron diffraction pattern of Cu_4O_x.

orderly fashion, which is different from the image of Cu_4O shown in the right-hand side of Fig. 2. Since such variation in contrast has taken place within several ångstroms, it can be ascribed to a change of the structure rather than to a variation of the sample thickness or the imaging conditions, as was done in the interpretation of the image of Cu_8O (Guan, Hashimoto & Kuo, 1984).

3.1. *The structure of* α-Cu_4O_x

The top part of Fig. 6 shows an HREM image of Cu_4O in the [001] orientation, where the bright spots represent the projections of the O atoms as reported previously (Guan, Hashimoto & Yoshida, 1984). The bottom part of Fig. 6 shows a magnified image of region *A* in Fig. 3, with the same magnification as for Cu_4O in the top image. By comparing both images it can be seen that the distances and the angles between the bright spots are the same, but the contrast of the spots is different in both figures, *i.e.* in the top image the contrast of the spots is uniform whereas in the bottom image it is alternately weak and strong, as indicated by the arrows between the two images.

Fig. 7(*a*) shows a projection of the structure of Cu_4O along [100], in which the small black dots represent the Cu atoms. The large circles represent the O atoms, and 0 and $\frac{1}{2}$ represent the heights of the O atom in the unit cell. Fig. 7(*b*) shows a projection of the structure of Cu_4O along [001], in which the large circles also represent the O atoms but the number 4 in the circles indicates that the O atoms are situated in the center of the tetrahedra formed by the Cu atoms. By comparing Figs. 7(*a*) and 7(*b*) it is seen that the large circles in Fig. 7(*b*) are the projections of the columns of the O atoms with respective heights of $a = 0$ and $\frac{1}{2}$ in Fig. 7(*a*). For the structure of Cu_4O, the density of the O atoms with respect to the heights 0 and $\frac{1}{2}$ is the same, so the intensities of the spots in the electron microscope image are the same as shown in the top part of Fig. 6, which is illustrated by the same arrows (1, 2, 3 and 4) between Figs. 7(*a*) and 7(*b*).

Considering the above discussion, projections of a trial structure of Cu_4O_x along the [100] and [001] directions were suggested as shown in Figs. 8(*a*) and 8(*b*). The projections in Figs. 8(*a*) and 8(*b*) are the same as those in Figs. 7(*a*) and 7(*b*), respectively. Comparing Figs. 7(*a*) and 8(*a*) it is seen that if the hatched circles in Fig. 7(*a*) are omitted, the figures are identical. From Fig. 8 it is seen that the basic periods of this model in the [010] and [001] directions are twice as large as those of Cu_4O. The basic period in the [100] direction stays the same as that of Cu_4O and this model explains the geometrical arrangement of the diffraction spots in Fig. 4.

According to this model, the number of O atoms in the unit cell can be counted and it is seen that the value of x is $\frac{3}{4}$, namely Cu_4O_x can be depicted as $Cu_4O_{0.75}$. For discrimination of this structure from the others shown later, it is named α-$Cu_4O_{0.75}$. From Fig. 8(*a*) we can see that the density of the O atoms with a height of 0 is less than that of the O atoms with a height of $\frac{1}{2}$ by a factor of two. This is illustrated by arrows 1, 2, 3 and 4 of different

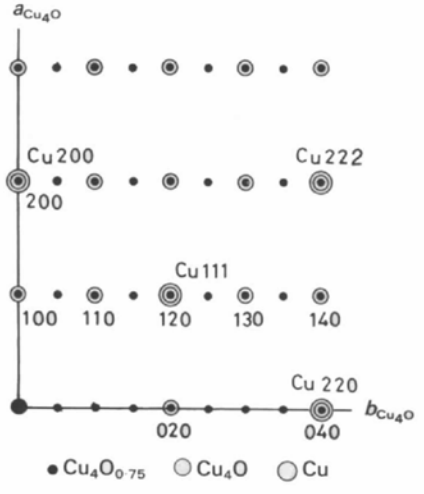

Fig. 5. Schematic diagram for comparison of the electron diffraction patterns of Cu_4O [001] and Cu_4O_x. Black dots represent the diffraction spots of Cu_4O_x, small circles represent those of Cu_4O and large circles Cu. The circles enclosing black dots indicate superposition.

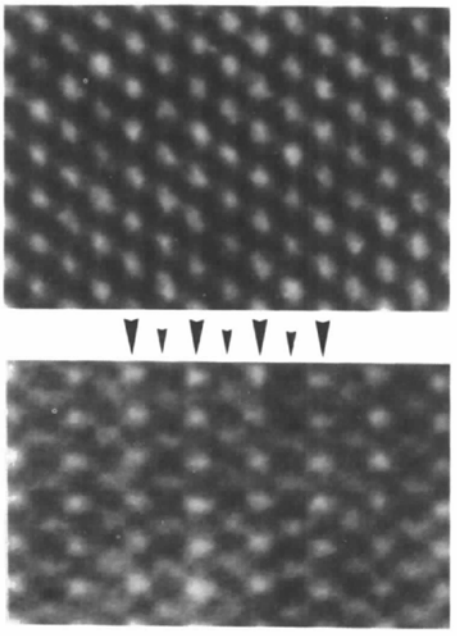

Fig. 6. Large-magnification images of Cu_4O_x from region *A* in Fig. 3 (bottom) and of Cu_4O projected along the [001] direction (top). Arrows: see text.

thickness between Figs. 8(*a*) and 8(*b*). In order to indicate this difference, the projections of the O atoms with a height of 0 and $\frac{1}{2}$ are shown in Fig. 8(*b*) by small and large circles, respectively.

In the present observations, only the electron micrographs and diffraction patterns projected along [001] Cu_4O were obtained. Thus the positions of the O atoms in the projection along [100] Cu_4O shown in Fig. 8(*a*) are only one of several possibilities. O atoms with 0 height in Fig. 8(*a*) can be the positions shown as A_1, A_2 or A_3, and those with $\frac{1}{2}$ height can be in positions B_1, B_2 or B_3, and B_1', B_2' or B_3'. Since the uniform distribution of O atoms in the copper lattice seems to be energetically stable, the model shown in Fig. 8(*a*) is reasonable, *i.e.* O atoms with 0 height are in the base center and those with $\frac{1}{2}$ height occupy the center position in (011) whose four corners are occupied by O atoms.

The model shown in Figs. 8(*a*) and 8(*b*) has been checked by comparison of the observed image contrast with calculations based on the dynamic theory of electron diffraction (multislice method) and HREM imaging theory. Fig. 9(*a*) shows the simulated images of [001] Cu_4O as reported earlier (Guan, Hashimoto & Yoshida, 1984). Figs. 9(*b*) and 9(*c*) show simulated images of α-$Cu_4O_{0.75}$ with two different thicknesses, and in the same [001] orientation as the image of Cu_4O. In the present calculation, partial coherence of the illuminating electron beam has been taken into account, *i.e.* the following parameters have been adopted: $C_s = 0{\cdot}7$ mm, $C_c = 1$ mm, $\Delta\alpha = 3 \times 10^{-3}$ rad, $\Delta = 15$ nm, $\Delta f = 200$ nm, $E = 100$ kV. The image contrast does not change until Δf becomes 230 nm, *i.e.* $\Delta f = 215 \pm 15$ nm produces images with the same contrast. It is also assumed that the number of excited waves in the crystals is 16384 and that the angle of the objective aperture is $g = 2\theta/\lambda = 5\ \text{nm}^{-1}$. The intensity of the bright spots in Fig. 9(*a*) is the same, which is in good agreement with that of the observed images shown in the top part of Fig. 6. The intensity of the bright spots in Figs. 9(*b*) and 9(*c*) changes regularly, which is also in good agreement with those of the observed images shown in the bottom part of Fig. 6. According to the simulated images shown in Figs. 9(*b*) and 9(*c*), it can be seen that the array of spots with stronger intensity corresponds to the projection of the O atoms at the height of $\frac{1}{2}$, which have a higher density of O in the atomic column along the illuminating beam direction; the array of less-bright spots corresponds to the projection of the O atoms at the

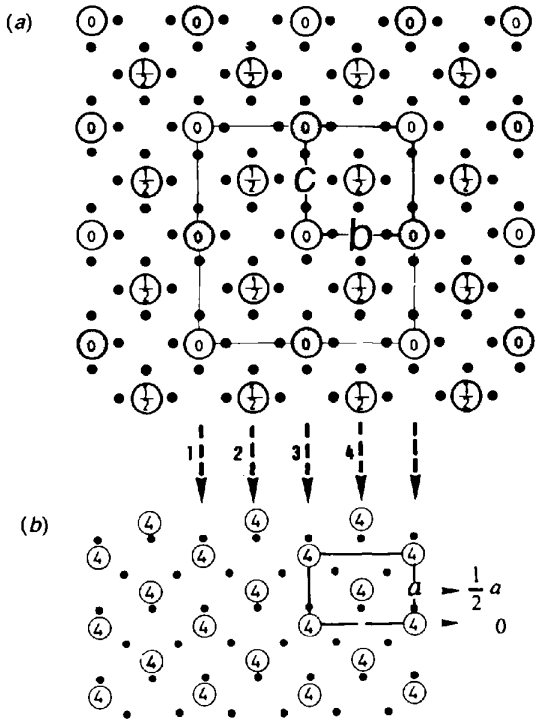

Fig. 7. Projections of the structure of Cu_4O along (*a*) [100] and (*b*) the [001] directions. The small square in (*a*) indicates the projection of the unit cell of Cu_4O. The large square in (*a*) corresponds to the square in Fig. 8(*a*). The arrows indicate the corresponding arrays of the O atoms in both figures.

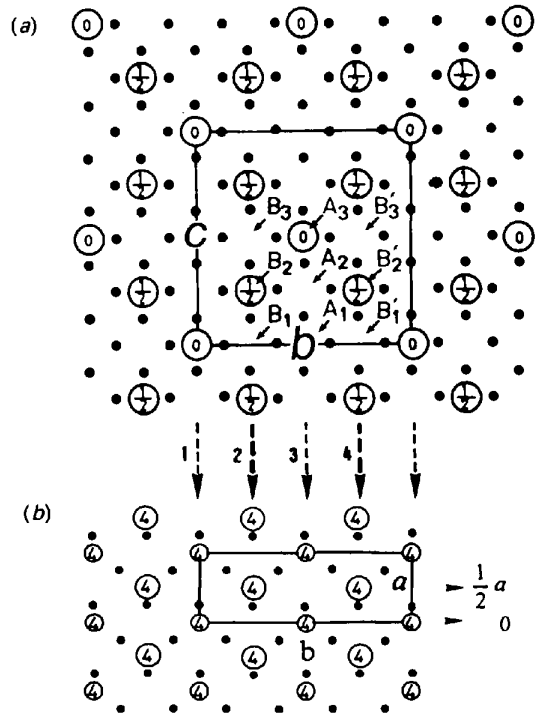

Fig. 8. Projections of the structure of α-$Cu_4O_{0.75}$ along (*a*) the [100] and (*b*) the [001] directions. The squares in (*a*) and (*b*) indicate the projection of the unit cell. The thick arrows (2 and 4) indicate the arrays with a higher density of O atoms and the thin arrows (1 and 3) indicate those with a lower density of atoms. A_1, A_2, A_3, B_1, B_2, B_3, B_1', B_2', B_3': see text.

height of 0 with a lower density of O atoms in the atomic column.

It is also seen that in the bottom image shown in Fig. 6 the weaker spots are laterally elongated. This may be caused by the variation of the film thickness, as confirmed by the simulated images shown in Fig. 9(*c*).

3.2. *The structure of* β-$Cu_4O_{0\cdot75}$

In order to interpret the features of the image shown in region *B* of Fig. 3, another structure model, named β-$Cu_4O_{0\cdot75}$, can be suggested as shown in Fig. 10. Fig. 10(*a*) is a projection of this structure along the [100] axis and Fig. 10(*b*) is that along the [001] axis. In this model, the positions of the O atoms along the [100] axis are at the heights of 0, $\frac{1}{4}$ and $\frac{3}{4}$, respectively, which can be ascertained from the image projected parallel to [001] shown in Fig. 3(*b*). It is seen that the distribution of the O atoms in each layer is the same as indicated by the three large squares in Fig. 10(*a*), but the arrangement of Cu atoms surrounding the O atoms in each layer is different. For example, the O atoms at the height 0 are situated in the octahedra of Cu atoms, but those at the heights $\frac{1}{4}$ and $\frac{3}{4}$ are situated in the tetrahedra, as shown by the numbers 4 and 8 in the circles in Fig. 10(*b*). The basic periods in the **b** and **c** directions are twice as large as those of Cu_4O, but in the [100] direction the basic period stays the same as that of Cu_4O. The number of O atoms is also less than that of Cu_4O by $\frac{1}{4}$, so the structure should be depicted as β-$Cu_4O_{0\cdot75}$. As described already, only the electron diffraction patterns and electron microscope images projected along [001] have been observed. From the intensity and position of bright spots in the electron microscope images, the height and number of O atoms projected along [100] can be speculated. As shown in Fig. 10(*a*), O atoms with height $\frac{1}{4}$ can be in the positions shown by A_1, A_2, $A_1 + c/2$, $A_2 + c/2$ and those with height $\frac{3}{4}$ in the positions B_1, B_2, $B_1 + c/2$, $B_2 + c/2$. Thus, a choice has to be made between positions A_1 or A_2 and B_1 or B_2. Since A_1 is closer to the O atoms with 0 height than A_2, A_2 may be the best possible position. The positions of B_1 and B_2 for the O atoms of $\frac{3}{4}$ height are equivalent, thus in the present model, the position B_1 has been adopted.

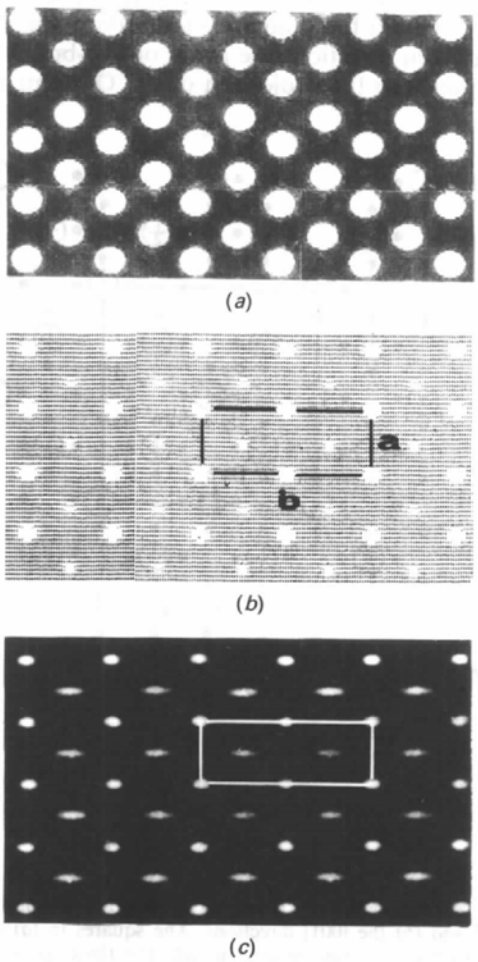

Fig. 9. Simulated images of (*a*) Cu_4O [001], (*b*) α-$Cu_4O_{0\cdot75}$ [001] (at a thickness of 6·5 nm) and (*c*) α-$Cu_4O_{0\cdot75}$ (at a thickness of 13·0 nm). $C_s = 0\cdot7$ mm, $C_c = 1$ mm, and $\Delta f = 200$ nm (see text).

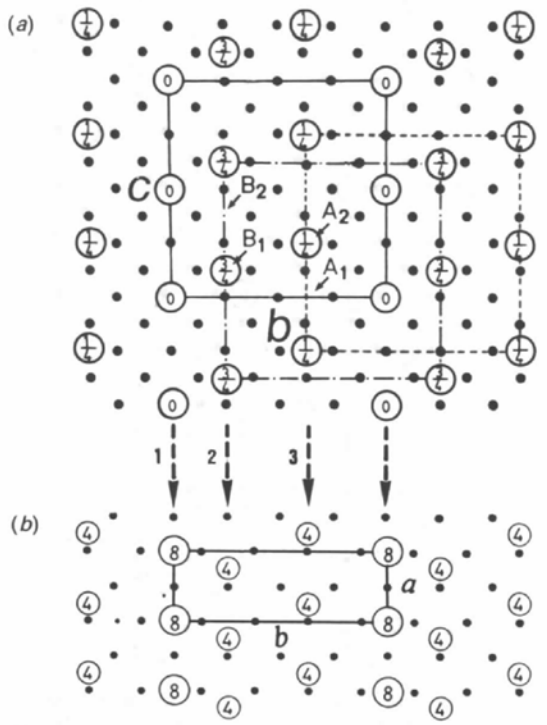

Fig. 10. Projections of the structure model of β-$Cu_4O_{0\cdot75}$ along (*a*) the [100] and (*b*) the [001] directions. The arrows indicate the corresponding arrays of O atoms. A_1, A_2, B_1, B_2: see text.

This model has also been confirmed by comparison of the observed and the calculated images shown in Fig. 11. The top part of Fig. 11 is a magnified image of region *B* of Fig. 3. The intensity difference of the bright spots in the observed image is more homogeneous than in α-$Cu_4O_{0\cdot75}$, but the spacing of the imaging spots is wider than that in α-$Cu_4O_{0\cdot75}$. The bottom part of Fig. 11 shows a simulated image with the same magnification as that of the top image; the simulated image was obtained on the basis of the structure model of β-$Cu_4O_{0\cdot75}$ shown in Fig. 10. A good agreement is obtained between the observed and the calculated images.

3.3. *The structure of* γ-$Cu_4O_{0\cdot75}$

Fig. 12 shows a structure model for the interpretation of the image shown in region *C* of Fig. 3. Fig. 12(*a*) is a projection of the structure model along the [100] axis and Fig. 12(*b*) is a [001] projection. In this model the O atoms at the height 0 are situated in the octahedra, but those at the heights $\frac{1}{4}$ and $\frac{3}{4}$ are in the tetrahedra, as shown by the numbers 8 and 4 in the circles in Fig. 12(*b*). It is seen from Fig. 12 that the density of the O atoms in the atomic column, indicated by the thick arrows 1 and 2, is twice as large as that in the arrays indicated by the thin arrows 3 and 4. The arrangement of O atoms is different from that in α- and β-$Cu_4O_{0\cdot75}$, and thus the structure is named γ-$Cu_4O_{0\cdot75}$. As discussed in §3.1 and 3.2, the positions and numbers of O atoms projected along [001] are deduced from the electron microscope images, but the projection along [100] is deduced from supposition. The O atom in base center with 0 height can be in the positions A_1, A_2, A_3, those with $\frac{1}{4}$ height in B_1, B_2, $B_1 + c/2$, $B_2 + c$, and those with $\frac{3}{4}$ height in positions C_1, C_2, C_3 (Fig. 12*a*). Since the atoms with $\frac{1}{4}$ height in B_1 or B_2 are equivalent, the atom with 0 height in A_1 or A_3 becomes equivalent and also energetically more possible than in A_2. Thus the possible models are of three kinds corresponding to the three positions of atoms with $\frac{3}{4}$ height, *i.e.* C_1, C_2 or C_3, as the position of atoms with $\frac{3}{4}$ height is not yet completely determined.

The top part of Fig. 13 is a magnified image of region *C* of Fig. 3. The features of this HREM image are as follows. Four kinds of bright-spot arrays are periodically distributed along the *b* axis. The intensity of the first array is strong, but the second, third and fourth arrays are weak. The bottom part of Fig.

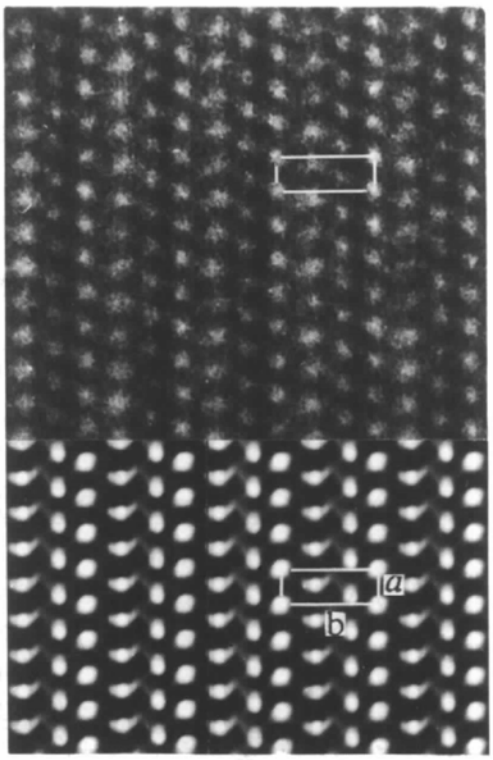

Fig. 11. Large magnification of the image shown in region *B* of Fig. 3 (top) and simulated image obtained on the basis of the structure model of β-$Cu_4O_{0\cdot75}$ [001] (bottom). Parameters used for the calculation are $t = 12\cdot6$ nm, $C_s = 0\cdot7$ mm, $C_c = 1$ mm, $\Delta f = 230$ nm, where t is the thickness.

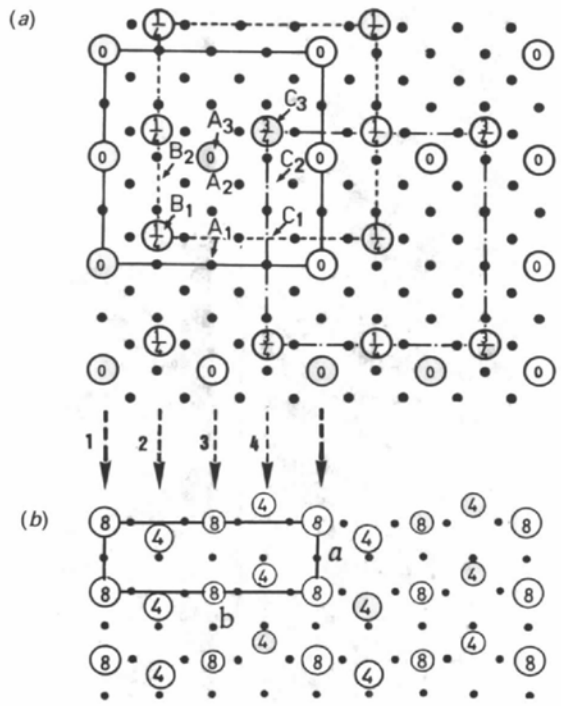

Fig. 12. Projections of the structure model of γ-$Cu_4O_{0\cdot75}$ along (*a*) the [100] and (*b*) the [001] directions. The arrows indicate the corresponding arrays of O atoms. Thickness of arrows, and number and size of the circles in (*b*): see text. A_1, A_2, A_3, B_1, B_2, C_1, C_2, C_3: see text.

13 is a simulated image with the same magnification as that of the top image; the simulated image was obtained on the basis of the [001] structure model of γ-$Cu_4O_{0\cdot75}$ shown in Fig. 12. It can be seen that the intensities of the simulated imaging spots are similar to those of the observed bright spots in the image. From the calculations it is known that the bright spots with strong intensity just correspond to the O atoms in the octahedra and in the atom columns with higher density of O atoms, whereas those with weak intensities correspond to those in the tetrahedra and in the columns with lower density of O atoms. From these coincidences, it can be concluded that the observed bright-spot image shown in region *C* of Fig. 3 represents the distribution of the O atoms of the model of γ-$Cu_4O_{0\cdot75}$ in the [001] orientation.

4. Discussion and conclusions

Three structural models, referred to as α-$Cu_4O_{0\cdot75}$, β-$Cu_4O_{0\cdot75}$ and γ-$Cu_4O_{0\cdot75}$, have been presented to interpret the HREM images shown in regions *A*, *B* and *C* of Fig. 3. Their lattice parameters are $a = 4\cdot02$, $b = 11\cdot34$, $c = 11\cdot88$ Å, and their crystal system is orthorhombic. These crystals are formed locally in the regions of 6 to 15 nm thickness of Cu_4O thin film of 300 nm^2 area and thus it is rather difficult to take images of these areas from more than two directions. However, by referring to the previous structure analysis of Cu_4O, Cu_8O and $Cu_{64}O$, and by studying the intensity distribution of the images of atoms projected onto the (001) plane, the most probable atomic structures of α-, β- and γ-$Cu_4O_{0\cdot75}$ have been obtained, although γ-$Cu_4O_{0\cdot75}$ has three possible models and requires further observations from different orientations before the correct model can be identified.

The fact that only the O-atom contrast appears in the HREM images of $Cu_4O_{0\cdot75}$ can be qualitatively understood from the standpoint of the thickness dependence of the amplitude of the diffraction waves as has been discussed already (Guan, Hashimoto & Kuo, 1986). Fig. 14 shows the film-thickness dependence of the amplitudes of the main diffracted waves in Cu_4O and α-, β- and γ-$Cu_4O_{0\cdot75}$. It is seen from

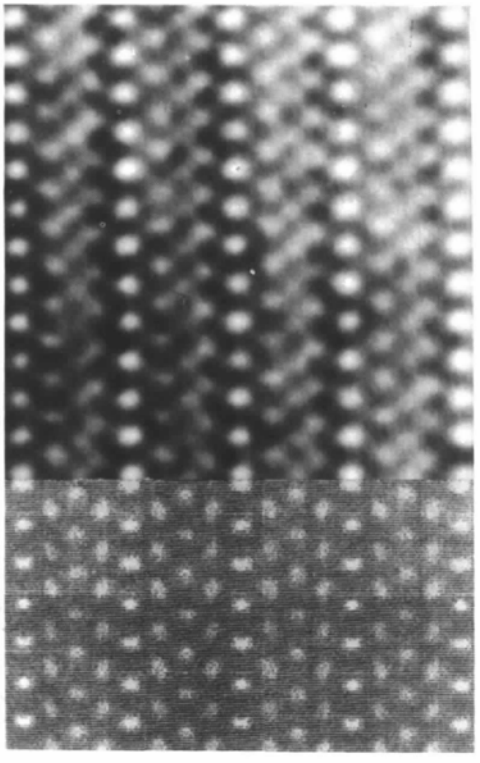

Fig. 13. Large magnification of the image of region *C* shown in Fig. 3 (top) and simulated image obtained on the basis of the structure model of γ-$Cu_4O_{0\cdot75}$ [001] (bottom). Parameters used for the calculation are $t = 13\cdot2$ nm, $C_s = 0\cdot7$ mm, $C_c = 1$ mm, $\Delta f = 230$ nm, where t is the thickness.

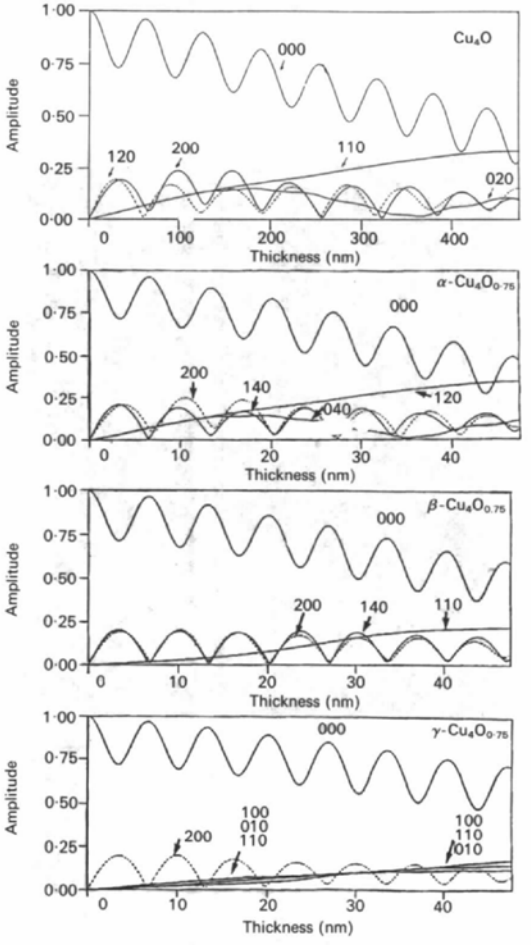

Fig. 14. Variations of the amplitudes of main reflections of Cu_4O [001], and α-, β- and γ-$Cu_4O_{0\cdot75}$ [001] with film thickness. Cu and O are assumed to be neutral atoms.

the structure of Cu_4O in Fig. 7(*b*) and that of α-$Cu_4O_{0.75}$ in Fig. 8(*b*) that the crystal planes (140) and (200) in α-$Cu_4O_{0.75}$ correspond to those of (120) and (200) in Cu_4O, which consist of Cu atoms, and the crystal plane of (120) in α-$Cu_4O_{0.75}$ corresponds to that of (110) in Cu_4O, which consists of O atoms. From Fig. 14 it can be seen that the amplitudes of the diffracted waves of (140) and (200) in α-$Cu_4O_{0.75}$, which reflect the periodicity of the arrangement of copper, vary with the film thickness at a periodicity of about 7 nm; in contrast, the amplitudes of the diffracted waves of (120), which reflect the periodicity of the arrangement of O, simply increase with the film thickness up to about 50 nm. Thus, when the film thickness becomes of a large-enough value, where the amplitude of (120) is larger than that of (140) and (200), the intensity of the imaging spots of O atoms will be stronger than those of Cu atoms. Similar arguments (based on Fig. 14 and the models shown in Figs. 10 and 12 respectively) hold for the structures of β- and γ-$Cu_4O_{0.75}$.

The present authors thank Drs M. Tomita and Y. Yokota and Mr Inada for their help in preparing this manuscript.

References

GUAN, R., HASHIMOTO, H. & KUO, K. H. (1984). *Acta Cryst.* **B40**, 560–566.
GUAN, R., HASHIMOTO, H. & KUO, K. H. (1985). *Acta Cryst.* **B41**, 219–225.
GUAN, R., HASHIMOTO, H. & KUO, K. H. (1986). *Ultramicroscopy*, **20**, 195–202.
GUAN, R., HASHIMOTO, H. & KUO, K. H. & YOSHIDA, T. (1987). *Acta Cryst.* **B43**, 343–346.
GUAN, R., HASHIMOTO, H. & YOSHIDA, T. (1984). *Acta Cryst.* **B40**, 109–114.

Acta Cryst. (1990). **B46**, 111–117

Electron Microscopy Study of the Incommensurately Modulated Structure of Ankangite

BY X. J. WU AND F. H. LI

Institute of Physics, Chinese Academy of Sciences, Beijing 100080, *People's Republic of China, and Beijing Laboratory of Electron Microscopy, Beijing* 100080, *People's Republic of China*

AND H. HASHIMOTO

Faculty of Engineering, Okayama University of Science, Okayama 700, *Japan*

(*Received* 10 *July* 1989; *accepted* 27 *November* 1989)

Abstract

The one-dimensional incommensurately modulated structure of ankangite $[Ba_{0.827}(Ti_{5.827}V_{2.294}Cr_{0.053})O_{16}]$, a mineral recently discovered in China, has been studied by electron diffraction and high-resolution electron microscopy. Its average structure is tetragonal with lattice parameters $a = 10.2$ and $c = 2.96$ Å and possible space groups $I4$, $I\bar{4}$ and $I4/m$. The modulated wave spreading along the c axis has wavelength $\lambda = 2.30c$. By referring to the results of the electron diffraction analysis it is suggested that the existence of a large number of vacancies inside tetragonal channels makes the Ba ions deviate from their idealized positions to form the modulated structure. Diffuse diffraction streaks passing through satellite spots were observed and hence modulation waves through adjacent Ba-ion strings are considered to be incoherent. This was confirmed by high-resolution electron microscopy and optical diffraction. The effect of electron-beam irradiation on the structure of ankangite is reported.

1. Introduction

Ankangite $[Ba_{0.827}(Ti_{5.827}V_{2.294}Cr_{0.053})O_{16}]$ is a new mineral recently discovered in China. Its chemical formula is close to that of priderite. The crystal structure of ankangite was also considered to be similar to that of priderite (Zhou & Ma, 1987), which is isomorphous to hollandite. The crystal structure of hollandite has been determined by X-ray diffraction (Bystrom & Bystrom, 1950, 1951). Fig. 1 shows a structure model of hollandite projected along the c axis (Bystrom & Bystrom, 1950). In the structure of hollandite MO_6 octahedra (where M represents Mn and its substitutes) share edges along the c axis, forming strings which are linked by corner-sharing and edge-sharing to form tetragonal channels with

0108-7681/90/020111-07$03.00